Stabbforsmo, T., and M. Tangstad. 2026. Hot Strength of β-SiC Produced from Biocarbon. In *Silicon for the chemical and solar industry XVIII*, edited by M. Tangstad, H. Rong, A. Valderhaug, B. Andresen, H. Dalaker, and I. G. Page. Kristiansand, Norway, September 7–10, 2026.
https://doi.org/10.55669/oa900809

Hot Strength of β-SiC Produced from Biocarbon

T. Stabbforsmo[1], and M. Tangstad[1]
[1] Norwegian University of Science and Technology, Department of Materials Science and Engineering, Norway, thea.stabbforsmo@ntnu.no

Keywords: biocarbon, charcoal, hot strength, SiC

Abstract - In the production of silicon metal, β-SiC is produced as a crucial intermediate product which occupy a significant part of the interior of the submerged arc furnace (SAF). β-SiC is produced by the reaction between carbon and SiO gas. This work investigates how the compressive hot strength of β-SiC is affected by the carbon precursors coal and charcoal. The compressive hot strength is measured indirectly by change in particle size distribution after being exposed to compressive forces at room temperature, 400 °C, 800 °C and 1000 °C in a Spark Plasma Sintering (SPS) machine. The strength of SiC from charcoal is found to be up to 50 % lower than calcined charcoal, while there is no significant difference between SiC from coal and calcined coal. This is suggested to be caused by the deterioration of the organized cell wall structure when reacting from charcoal to SiC, while the coal has thicker cell walls and is not affected by SiC conversion in the same degree. It is also found that the strength of SiC from charcoal is more temperature dependent than SiC from coal, with an increase in strength at 800 °C and 1000 °C, while SiC from coal shows approximately the same strength for all temperatures. As expected, the strength of SiC from coal is significantly higher than of SiC from charcoal.

1. INTRODUCTION

A potential approach to reduce the carbon footprint of the silicon industry is to exchange some of the fossil carbon material with renewable biocarbon in the charge, as this can reduce the CO_2 emission factor (Monsen, Lindstad and Tuset, 1998). Silicon metal production is a carbothermic process where a mix of various carbon materials reduce quartz (SiO_2) in a submerged arc furnace (SAF). The process involves a series of reactions leading to the total mass balance described in Equation 1.

$$SiO_2\ (s) + 2C\ (s) = Si\ (l) + 2CO\ (g) \quad [1]$$

One of the reactions leading to the mass balance in Equation 1 is the reaction between SiO gas from the inner zone in the SAF rising to the outer zone where it reacts with the carbon material to form silicon carbide (SiC) and CO gas, as described in Equation 2.

$$SiO\ (g) + 2C\ (s) = SiC\ (s) + CO\ (g) \quad [2]$$

The SiC produced by Equation 2 is essential for the production of Si metal, as it is the intermediate SiC which reacts with SiO gas to form molten Si and CO gas in the inner part of the furnace, as described in Equation 3.

$$SiO\ (g) + SiC\ (s) = 2Si\ (l) + CO\ (g) \quad [3]$$

It is well established that biocarbon materials such as charcoal generally have has lower mechanical strength than fossil carbon materials such as coal and coke. It is less established how the SiC strength is compared to the carbon materials, and how the strength is affected by the carbon precursor, especially at the high temperature inside the SAF. The SiC produced by Equation 2 is β-SiC if the temperatures are below 2000 °C, but it has been observed that with

exposure to temperatures above >~2000 ℃ β-SiC will convert to α-SiC (Ringdalen, 2018; Jayakumari and Tangstad, 2020). During excavation of five different Si furnaces, SiC was found in all furnaces (Ksiazek, Tangstad and Ringdalen, 2016). Ringdalen looked into the formation of α-SiC and β-SiC in industrial furnaces and found the loose charge at the top of Si furnaces to contain only β-SiC, while the SiC crust from further down in the furnaces contained a higher amount of α-SiC, with only small amounts of β-SiC or no β-SiC at all (Ringdalen, 2018). A crust of SiC was found to occupy up to almost half the interior of a 40 MW SAF at Elkem Thamshavn, although this is a more extreme case, it emphasizes the importance of knowledge of how this material is affected by the charge materials (Ksiazek, Tangstad and Ringdalen, 2016).

SiC is widely known for its many desirable properties, including high strength and chemical stability, making it suitable for a wide range of applications, especially as an abrasive medium. It is commonly produced through the Acheson process, but it can also occur naturally, then known as Moissanite. There are several polytypes of SiC, which can be classified as β-SiC or α-SiC, the latter being the most commercially used. Polytypes are named by a number and a letter, such as the cubic 3C β-SiC polytype. Other common polytypes include the hexagonal 4H, 6H and 8H as well as the rhombohedral 15R, which are all α-SiC polytypes. It has been suggested that β-SiC is the non-equilibrium product, existing up to 2750 ℃, while 2H and 6H are the main polytypes at temperatures lower than 2750 ℃ when the system is in equilibrium, which is in accordance with the findings of Jayakumari (Jayakumari and Tangstad, 2018; Jayakumari, 2020).

Kim et al. looked into how mechanical properties of porous SiC ceramics are affected by the Si/C content (Kim *et al.*, 2020). The SiC ceramics they used were made from β-SiC and carbon black, forming a SiC ceramic consisting of the β-SiC polytype 3C and α-SiC polytypes 6H and 4H, as well as some Si at the highest Si content (30 wt%). Their results indicate that a higher carbon content increases strength in porous SiC ceramics up to 5 wt% carbon, with a decrease in strength with further increased carbon content. A compressive strength of 100 MPa at 0% carbon with an increase to 106.4 MPa at 5 wt% carbon was measured, followed by a decrease in compressive strength with higher wt% C, to 12.5 MPa with 30 wt% C addition. The opposite was observed for addition of Si, where it increased from 7.7 MPa at 0 wt% Si addition to 24.6 MPa after addition of 30 wt% Si. This indicates that a higher Si/C ratio can increase the strength of porous SiC ceramics, and is in line with the findings of Hoover (Hoover, 2023). Hoover tested the cold compressive strength of SiC from coal with different degrees of conversion, and found that the strength of coal slightly decreased with increasing SiC amount, until Si started to form, also indicating that a higher Si/C ration can increase the strength in more disordered SiC materials (Hoover, 2023).

There are concerns related to the higher friability of biocarbon than fossil carbon, particularly due to issues related to the generation of fines (Ramos *et al.*, 2019; Jahrsengene *et al.*, 2023). Higher friability can lead to a larger generation of fines, which can cause a series of problems such as mass loss, HSE issues related to inhalation and the risk of dust explosions, as well as negative effects on furnace operation and limited gas flow (Jahrsengene *et al.*, 2023). When charcoal reacts with SiO gas to form SiC, it is a topochemical reaction following the shrinking unreacted core model, i.e. SiO gas reacts on the surface of the pores and diffuses into the material, first transforming the pore walls to SiC (Jayakumari, 2020). The mechanical strength of carbon materials is dependent on the porosity and cell wall thickness, as it is the cell walls which are load bearing. The higher porosity and thinner cell walls in charcoal are therefore key factors contributing to charcoals lower strength compared to coal and coke. The literature on the extent of precursor effect on strength and friability of SiC in Si production is limited.

However, Hoover looked into the compressive strength of SiC made from coal and char, where the strength of SiC from coal slightly decreased with increasing SiC content, while the opposite trend was observed for SiC from char (Hoover, 2023). The strength of SiC from both coal and char were measured to be significantly lower than reported for commercial β-SiC.

As there is a knowledge gap in the hot strength of β-SiC as an intermediate product from biocarbon in Si production, it must be examined before charcoal is implemented on a larger scale. In this work the hot strength of SiC from coal and charcoal is investigated by the application of a Spark Plasma Sintering (SPS) machine, which can both heat samples and apply force. The effect of conversion to SiC is examined by density and porosity measurements, Scanning Electron Microscope (SEM) and Energy-Dispersive X-ray Spectroscopy (EDS), X-ray Diffraction (XRD), as well as μ-Computed Tomography (μ-CT).

2. METHOD

SiC was produced from calcined (1200 ℃ for 20 minutes) coal and charcoal, with the proximate composition shown in Table I, with calcined coal having a slightly higher fix-C than calcined charcoal.

Table I: Proximate analysis of calcined coal and charcoal (1200 ℃ for 20 minutes) on a dry basis, used for production of SiC.

	Fix-C (%)	Volatiles (%)	Ash (%)
Charcoal	93.1	3.2	3.7
Coal	97.8	0.8	1.3

With inspiration from the work of Jayakumari, the SiC was produced in a setup in an Inductotherm 75 kW furnace (Jayakumari, 2020). The setup was based on an BN coated graphite crucible (150 x 114 x 400 mm). The bottom of the crucible contained a mixture of Si and SiO_2. Three BN coated graphite pillars were also placed in the bottom of the crucible as a fundament for the graphite sieve separating the SiO producing materials from the carbon material, as shown in Figure 1a. The graphite sieve was 5 mm thick and approximately 110 mm in diameter. To allow for high gas flow upwards in the crucible the sieve was covered in holes as shown in Figure 1b. The carbon material was placed above the sieve together with a BN coated graphite tube (20 x 8 x 500 mm) which contained an alumina tube with a C-type thermocouple which measured the temperature inside the crucible during the process, as seen in Figure 1c.

a) b) c)

Figure 1: The different layers in the SiC formation set-up in the BN coated graphite crucible. Showing a) Si + SiO_2 mix and BN coated graphite pillars. b) The BN coated graphite sieve separating the Si + SiO_2 mix from the carbon material. c) Charcoal on top of the sieve and the BN coated closed-end graphite tube for the thermocouple.

The process was based on the reaction between SiO_2 and Si in the bottom of the crucible, which produce SiO gas, according to Equation 4.

$$SiO_2 + Si = 2SiO\ (g) \qquad [4]$$

The SiO gas produced in the bottom of the crucible rose through the sieve, to the carbon material where it reacted to form SiC and CO gas, as described in Equation 2. The process was carried out at ~1800 ℃ with a holding time of 60 minutes, and a heating rate of approximately 50 ℃/min. The amount of coal and charcoal differed between 200 g and 400 g. After cooling, the materials above the sieve were manually sorted according to conversion degree based on colour as shown in Figure 2, where the greenest material is the most converted. All materials from the same carbon material categorized as the most converted were mixed, and the most converted materials were further investigated and hot strength tested.

Figure 2: Sorting degree of SiC conversion from charcoal/coal manually by colour. The green/grey material closest to the camera is the most converted SiC.

Chemical analysis was carried out at Degerfors Laboratorium, where the amount of SiC in the samples was calculated based on Si detected in the samples, assuming that the amount of elemental Si present is negligible. The conversion degree of the most converted SiC from charcoal and coal was found to be 99 % and 52 %, respectively. Powder X-ray Diffraction (XRD) with Rietveld refinement for phase quantification of the SiC samples was also carried out using the software TOPAS. How well the refinement fit the XRD diffractogram is quantified by the "Goodness of fit" (GOF), where a lower GOF equals a better fit. Before XRD the samples were crushed and sieved through a 44 µm sieve. Cu-Kα radiation (λ = 1.5406) was applied in Bragg-Brentano geometry, with a measurement time of 120 minutes between 2θ = 20-80°.

Hot strength was measured with the application of a Spark Plasma Sintering (SPS) machine, which can steadily heat a sample and apply force. The procedure is the same as described in greater detail in (Stabbforsmo and Tangstad, to be published). The batch of material for the most converted SiC was split with a splitter to ensure representative samples. A material bed of approximately 1.5 g 4-6.3 mm SiC particles was placed in the 28.4 mm graphite die between two graphite punches. The inside of the graphite die is covered by graphite paper, as well as the ends of the graphite punches in which the sample is placed between. The

punches were secured by a manual press before it was placed in the SPS. The graphite setup was covered in graphite wool before hot strength testing. The testing temperatures were 25 ℃, 400 ℃, 800 ℃ and 1000 ℃, and a K-type thermocouple was used. The heating rate was 25 ℃/min up to 400 ℃ and 15 ℃/min above 400 ℃ to minimize rapid expansion of crucible causing premature compression of the sample. The minimum constant force during heating was 2 kN, and a total force of 4 kN with a rate of 0.65 kN/min was applied to the sample when the goal temperature was reached. Two parallels were carried out per sample at each temperature. After the samples had been subjected to compression at the various temperatures, the particle size distribution was measured by sieving. The particle size distribution after compression at elevated temperatures was used to evaluate the hot strength of the material. The same method was also used to measure the hot strength of calcined coal and charcoal as also presented in (Stabbforsmo and Tangstad, 2026).

Absolute density, also known as material density or particle density, was measured by helium pycnometry with the use of an Accupyc 1340. The apparent density was measured by SINTEF Industry by sand with the use of a Geopyc 1360. Porosity was calculated by Equation 5.

$$Porosity\ (\%) = 1 - \frac{Apparent\ density}{Absolute\ density} \quad [5]$$

Scanning electron microscopy (SEM) and energy dispersive spectroscopy (EDS) was carried out on the samples with the use of a Jeol IT800 to examine the morphology of the samples, as well as the extent and way of reaction to SiC. SEM images were also used to measure the cell wall thickness of samples of calcined charcoal and SiC from charcoal.

The interior of SiC from charcoal and coal was investigated by μ-CT, with the use of a Nikon XTH 225 ST Microfocus CT in reflection mode with Tungsten target.

3. RESULTS AND DISCUSSION

The ability to withstand compressive forces without breaking can be related to the strength of the material. The results in Figure 3 and Figure 4 show a larger amount of small particles after hot strength testing of SiC from charcoal than calcined charcoal. This indicate that SiC from charcoal has significantly lower hot strength than calcined charcoal at all testing temperatures. The hot strength decreases by ~50 % when calcined charcoal is converted to SiC, when comparing the mass of particles >3.15 mm at 1000 ℃. Both calcined charcoal and SiC from charcoal increase in strength at 800 ℃ and 1000 ℃, indicating that the strength increases with increasing temperature.

Figure 3 and Figure 4 show that the particle size distribution after compression at the elevated temperatures SiC from coal is approximately the same as for calcined coal at all temperatures, but it does not increase in strength at 1000 ℃ unlike calcined coal. This indicates no significant change in strength from calcined coal to 52 % SiC from coal. Though Hoover claimed a small difference in strength, this seems to be within the uncertainty of the measurements and in line with these findings (Hoover, 2023). The hot strength of SiC from coal is significantly higher than of SiC from charcoal at all temperatures, as expected.

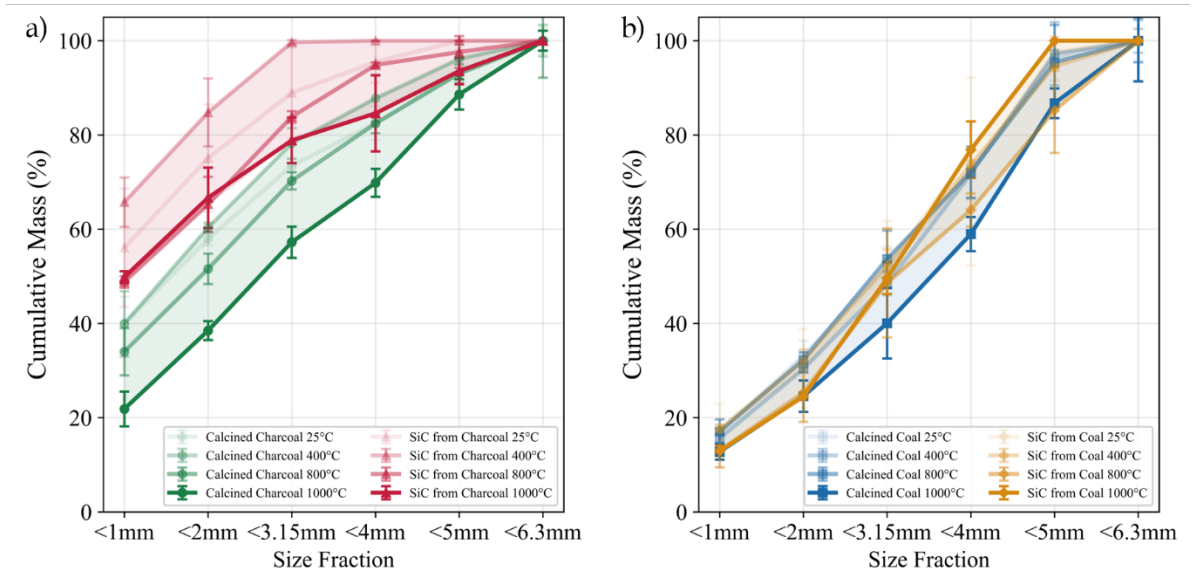

Figure 3: Cumulative mass for a) SiC from charcoal (red) and calcined charcoal (green) and b) SiC from coal (orange) and calcined coal (blue) after hot strength testing in the SPS.

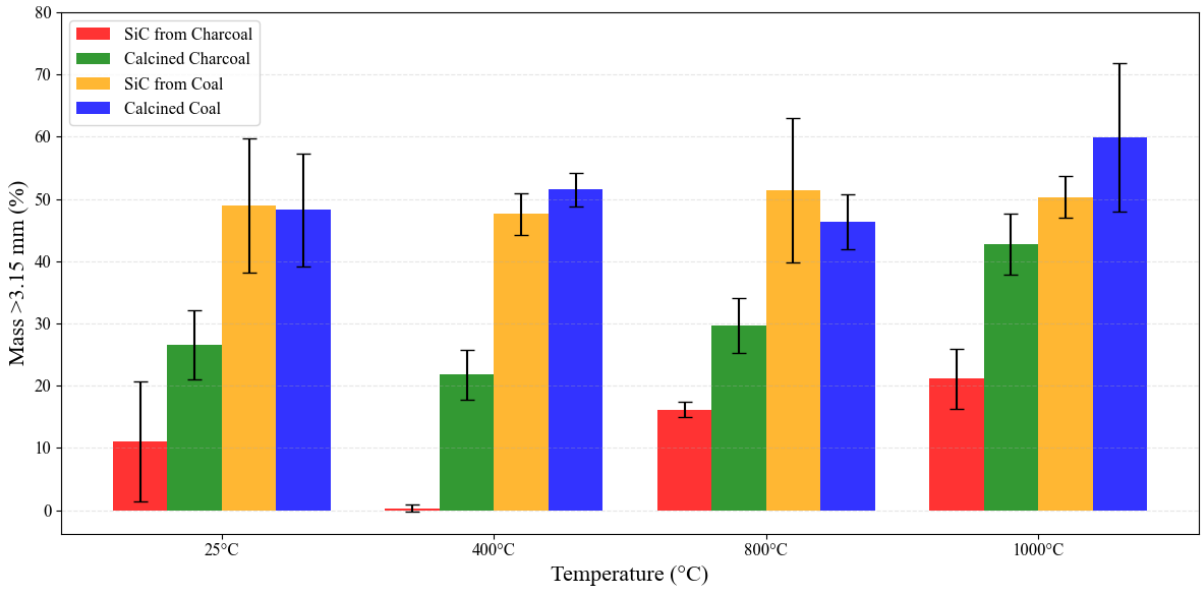

Figure 4: Total mass of particles >3.15 mm after hot strength testing in SPS, showing the difference in strength in SiC from coal and charcoal and calcined coal and charcoal. Values for calcined coal and charcoal also found in (Stabbforsmo and Tangstad, 2026).

The significant decrease in strength with the transformation from charcoal to SiC is likely linked to thinning of cell walls and decrease in structural integrity when charcoal reacts with SiO gas to form SiC, as seen in the SEM images in Figure 5. Measurements of cell wall thickness indicate a slight decrease in cell wall thickness with the transformation to SiC from calcined charcoal, with an average of 1.7 ± 0.5 µm cell wall thickness for calcined charcoal and 1.2 ± 0.3 µm for SiC from charcoal. It is mainly the cell walls that are load bearing, and when they lose their integrity the strength decreases. Figure 5a also show that some of the SiC produced deposits inside the pores. The SiC crystals appear to be loosely packed, which in combination with thinning of cell walls likely contributes to the decrease in mechanical strength with the conversion of charcoal to SiC.

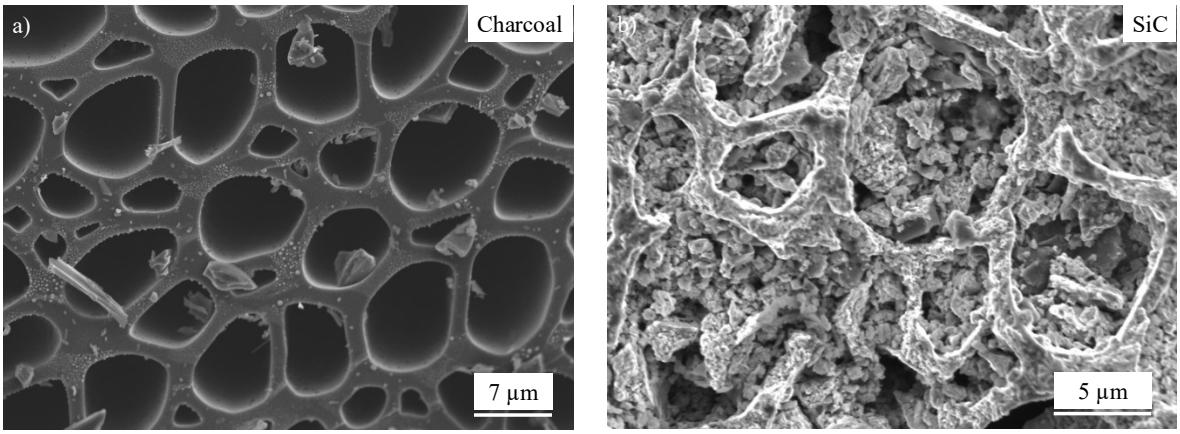

Figure 5: SEM images of a) SiC from charcoal showing the SiC crystals formed from the pore walls and b) calcined charcoal.

The strength of the materials is also usually also related to the porosity. As shown in Figure 6a, the average porosity of SiC from charcoal is found to be slightly lower than for calcined charcoal (81 % to 77 %), but as the margin of error is large the change is not considered to be significant and does likely not have a big effect on the strength of the material. The change in porosity with the reaction to SiC from coal is slightly more significant (61 % to 66 %) as the margin of error is smaller, but it is likely too small to contribute to a decrease in strength as this is not observed. A decrease in porosity with reaction to SiC is expected due to SiC having a larger molar volume than C, thus occupying more space. This is the opposite as observed for SiC from coal, but it can possibly be explained by the formation of CO gas from the reaction between SiO and C to SiC. CO generation can create a local increase in partial pressure if it cannot escape easily. Calcined coal is denser than charcoal, which can cause a local pressure build up leading to the growth of pores before it diffuses out of the material. Calcined charcoal already has a lower density and higher porosity which enable rapid gas escape and prevents pressure build up, thus also further porosity development. As expected, the absolute density of the material from both coal and charcoal increases with the conversion to SiC, as seen in Figure 6b. The theoretical density of 3C SiC is 3.2 g/cm^3 (Gavrilov, 1978), while the absolute density of 99 % SiC from charcoal is measured to be 3.0 g/cm^3.

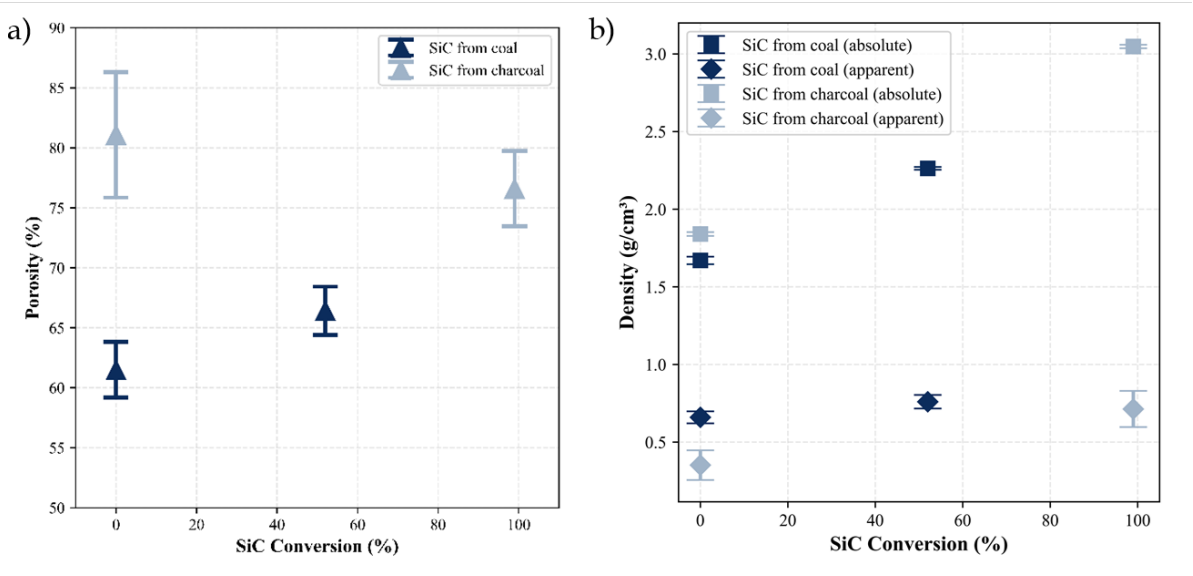

Figure 6: Measured a) porosity, and b) apparent density and absolute density of calcined coal and charcoal, as well as SiC from coal and charcoal. Values for calcined coal and charcoal from (Stabbforsmo and Tangstad, 2026).

The reaction between carbon particles and SiO gas to form SiC is observed to be topochemical, following the shrinking unreacted core model as seen in the image of a partly converted SiC particle from charcoal in Figure 7. The image shows a black core of charcoal and an outer layer of SiC, as expected. The composition of the layers was confirmed by EDS mapping as shown in Figure 8b. The reaction is also seen to occur in the large, open pores first, as green/grey dots are observed in the outer area of the charcoal core in Figure 7.

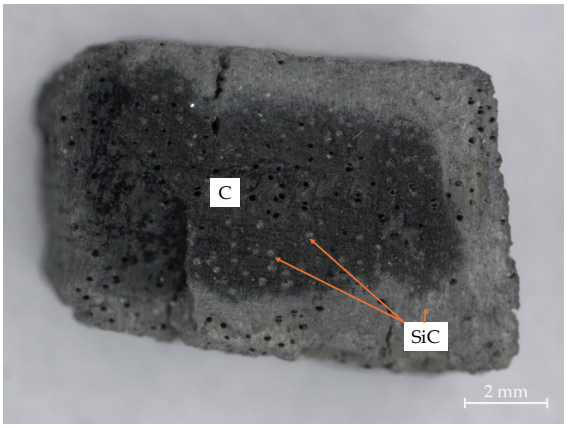

Figure 7: Image of the fracture surface of the interior cross-section of a partly converted SiC particle from charcoal. The particle reacts from the outer surface towards the centre, following the shrinking unreacted core model. Orange arrows indicating SiC as an outer layer as well as in pores in the carbon core.

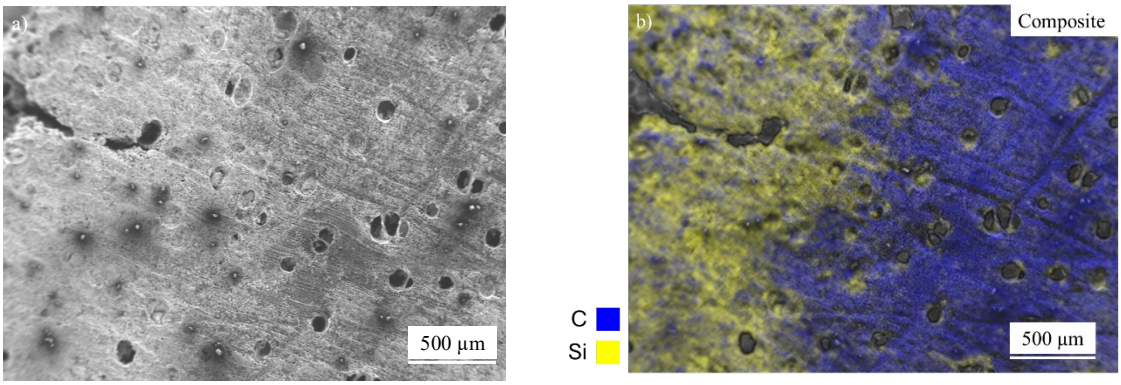

Figure 8: a) SEM image of the cross-section of a partly converted charcoal sample. b) EDS composite map of the area of transition from C to SiC showing carbon and silicon. The overlapping yellow and blue on the left indicates SiC and the blue is carbon (charcoal) on the right.

SiC crystals and whiskers were observed on the surface of particles of SiC from coal as seen in Figure 9a, b and c. This is confirmed by EDS point analysis carried out at the three points marked in Figure 9c, indicating approximately 50 at% carbon and 50 at% Si as listed in Table II. This is in line with the observations of others when converting carbon materials to SiC (Jayakumari and Tangstad, 2020; Hoover, 2023). Figure 9d shows the unreacted core of a sample of SiC from coal.

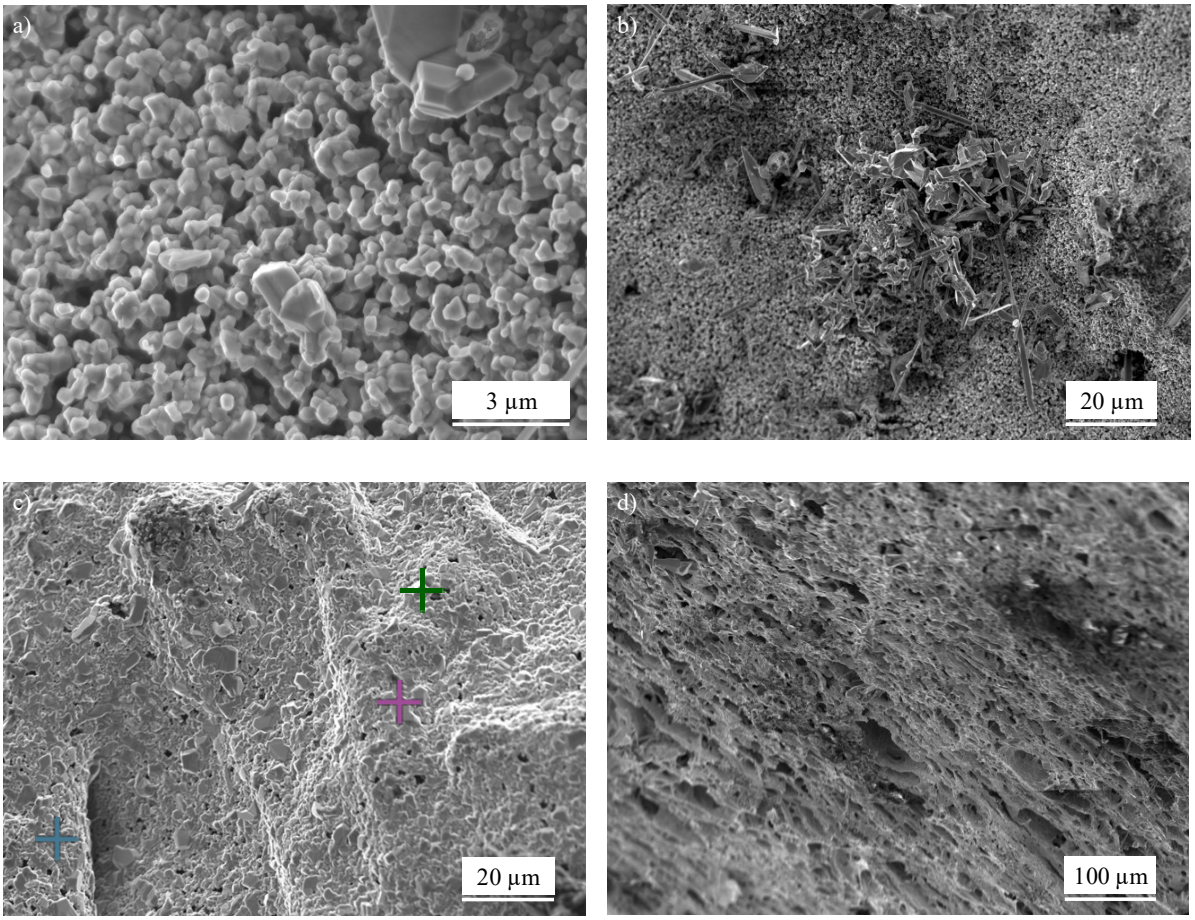

Figure 9: a) b) and c) shows the surface of a sample of SiC from coal with SiC crystals at different scale. b) shows SiC crystals and whiskers. In c) the green, pink and blue marks shows the spots for EDS point analysis and d) interior fraction surface of SiC from coal showing significant porosity and not small SiC crystals as on the surface.

Table II: Average atomic percent of C and Si detected by EDS point analysis at the three points shown in Figure 9c, indicating SiC.

	Average C (at%)	**Average Si (at%)**
SiC from coal	49.99 ± 2.57	50.01 ± 2.57

The XRD analysis shown in Figure 10 and Table III indicates a larger presence of amorphous graphite in the SiC from coal and very small amounts in the SiC from charcoal, in line with the chemical analysis. The main SiC polymorph is β-SiC, but there are also small amounts of an uncertain α-SiC polytype (2H was used in the refinement), along with ~1 % elemental Si in the SiC from charcoal, as presented in Table III. This is in line with the findings from SEM and EDS, as well as inside the margins of uncertainty of the chemical analysis.

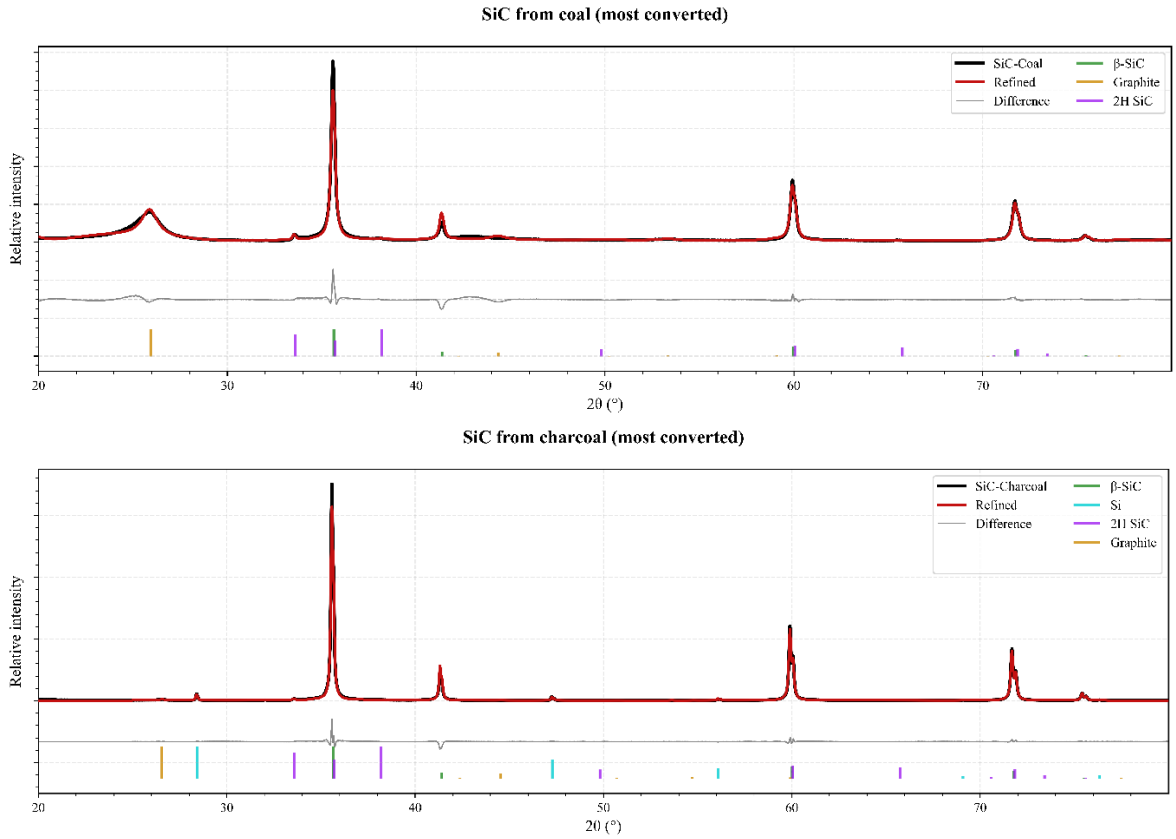

Figure 10: XRD diffractogram with Rietveld refinement for SiC from coal and charcoal, including the difference between the scan and refinement and bars for present structures. GOF for refinement is 7.97 for SiC from coal and 4.76 for SiC from charcoal. The present phases are indicated by the bars below the diffraction lines, they are β-SiC (green, PDF 04-008-4949, (Gavrilov, 1978)), graphite (orange, PDF 04-015-2407, (He *et al.*, 2007)) and 2H (purple, PDF 04-008-2392, (Sokhor and Glukhov, 1965)) for the most converted SiC from coal and β-SiC (green, PDF 01-075-0254, (Burdick and Owen, 1918)), Si (cyan, PDF 04-006-2527, (Steele and Rosi, 1958)), 2H (purple, PDF 04-008-2392, (Sokhor and Glukhov, 1965)) and amorphous graphite (orange, PDF 04-006-5764, (Zhao and Spain, 1989))

Table III: Quantitative analysis of phase content in the most converted SiC from coal and charcoal by Rietveld refinement from XRD. GOF for SiC from coal is 7.97 and 4.76 for SiC from charcoal.

	β-SiC (wt%)	**α-SiC (wt%)**	**Amorphous graphite (wt%)**	**Si (wt%)**
SiC from coal	47	<1	53	-
SiC from charcoal	97	<1	1	2

The μ-CT images in Figure 11 shows areas of different brightness. The lighter areas are of higher density and most likely consist of SiC, while the darker areas of lower density are unreacted carbon. The brightness and contrast of the images have been adjusted to make the particles the most visible. As the images are comparable with these adjustments, it indicates that the most converted samples have a higher density as they are significantly lighter. The lighter areas around the edge of the sample seen in Figure 11a likely consist of SiC while most of the samples in Figure 11b are converted to SiC. The findings of SiC around the edge of the material is in line with previous findings on SiC formation from carbon and SiO gas (Jayakumari and Tangstad, 2020), as well as the SEM and EDS shown in Figure 7 and Figure 8. Figure 11b also shows some smaller areas that are even lighter in some of the samples, especially in or around the pores, which could be Si as found by XRD.

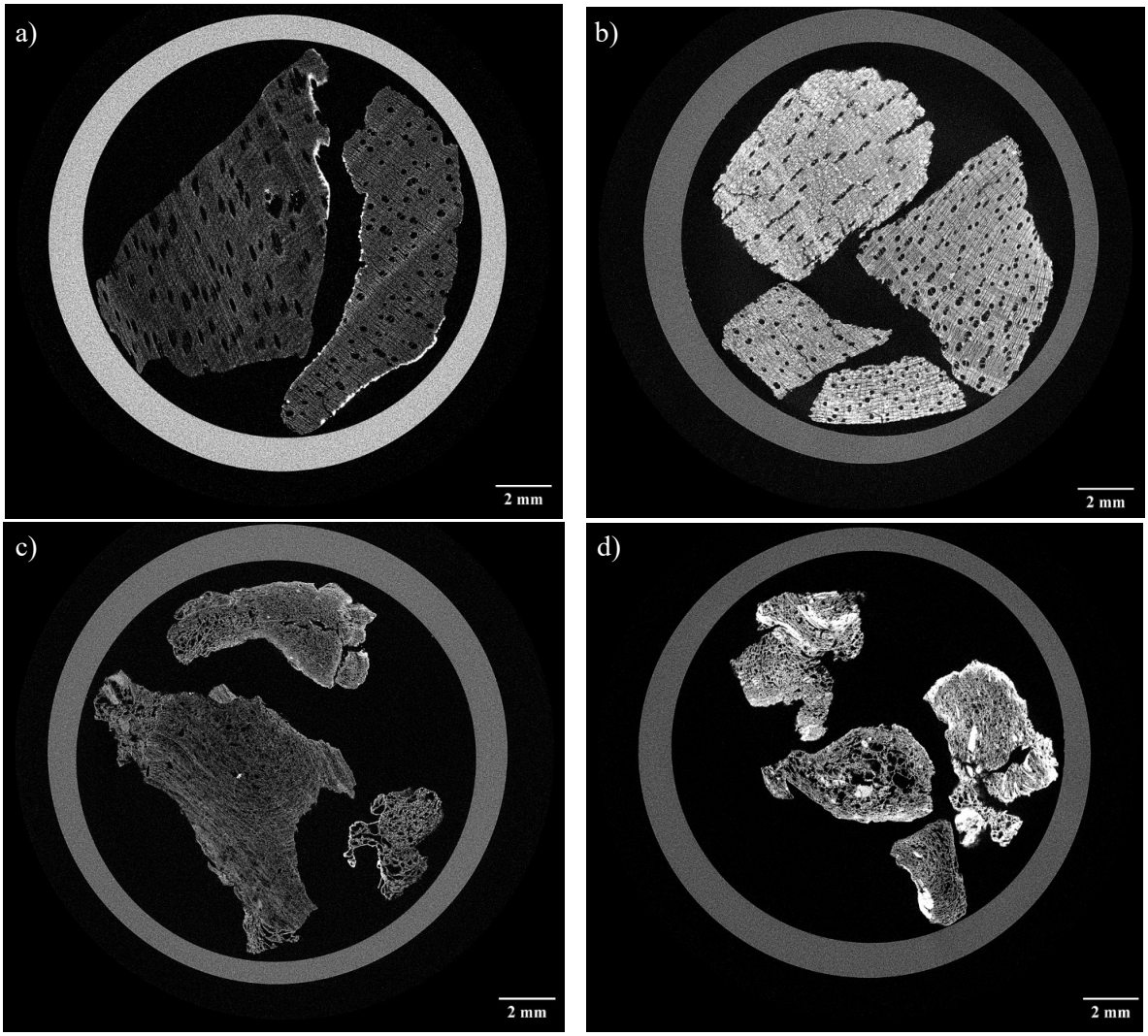

Figure 11: μ-CT images of a) 26 % SiC from charcoal, b) 99 % SiC from charcoal, c) 6 % SiC from coal and d) 52 % SiC from coal. Lighter areas have higher density and darker areas have lower density.

4. CONCLUSION

1. The hot strength of SiC from charcoal is significantly lower than of calcined charcoal, with ~50 % decrease in the distribution of particles >3.15 mm at 1000 °C. Likely due to the structural integrity of the material being compromised when the carbon from the cell walls react to form SiC. Both calcined charcoal and SiC from charcoal shows higher mechanical strength at 800 °C and 1000 °C than at lower temperatures.
2. The strength of SiC from coal is approximately the same as for calcined coal. For SiC from coal, the strength is found to be approximately the same at all temperatures, while calcined coal shows slightly higher strength at 1000 °C.
3. SiC from coal has, as expected, a significantly higher hot strength than SiC from charcoal at all temperatures. The difference in effect of SiC conversion on strength in charcoal and coal is likely to be affected by the difference in degree of conversion. The most converted SiC from coal contains 52 % SiC, while the most converted SiC from charcoal contains 99 % SiC. An important factor may also be the structure of the carbon precursor. Charcoal consists of an ordered structure of pores and thin cell walls, which the strength is highly dependent on. Coal on the other hand has lower porosity, higher density and thicker cell walls. This likely makes the integrity and strength of the coal less affected by the conversion to SiC than charcoal.

5. ACKNOWLEDGEMENT

This project has been financially supported by the Research Council of Norway through FME ZeMe, project number 350325.

6. REFERENCES

Burdick, C.L. and Owen, E.A., 1918. The atomic structure of carborundum determined by X-rays. *Journal of the American Chemical Society*, Vol.40, Issue 12, pp.1749–1759. https://doi.org/10.1021/ja02245a001.

Gavrilov, K.I., 1978. Variation of tetragonal bonds deformation in silicon carbide crystals with their hexagonality and degree of doping with nitrogen. *Sov. Phys. Crystallogr.*, Vol.23, Issue 6, pp.691–693.

He, J.L., Shen, Z.Q., Wu, E., Liu, Z.Y., He, L.L., Yu, D.L., Guo, L.C., Wu, Q.H., Luo, X.G. and Hu, Q.K., 2007. Carbon-rich boron carbide in the eutectic product synthesized by resistance heating of B2CN in graphite. *Journal of alloys and compounds*, Vol.437, Issue 1, pp.238–246.

Hoover, H., 2023. *Electrical Resistivity of Materials in the Silicon Furnace*. Doctoral thesis. NTNU.

Jahrsengene, G., Jayakumari, S., Kero, I.T. and Ringdalen, E., 2023. Sustainable Metal Production: Use of Biocarbon and the Concern of Dusting, COM 2023, *The 62nd Conference of Metallurgists*, Toronto, Canada, 21-24 August 2023, pp.1001-1007. https://doi.org/10.1007/978-3-031-38141-6_126.

Jayakumari, S., 2020. *Formation and characterization of β-and a-Silicon Carbide produced during Silicon/Ferrosilicon process*. Doctoral thesis. NTNU.

Jayakumari, S. and Tangstad, M., 2018. Formation of elemental silicon in β-SiC particles, *Silicon for the Chemical and Solar Industry XIV*, Svolvær, Norway, 11-14 June 2018, pp.125–138.

Jayakumari, S. and Tangstad, M., 2020. Transformation of β-SiC from Charcoal, Coal, and Petroleum Coke to α-SiC at Higher Temperatures. *Metallurgical and Materials Transactions B*, Vol.51, Issue 6, pp.2673–2688. https://doi.org/10.1007/s11663-020-01970-1.

Kim, G.-D., Kim, Y.-W., Song, I.-H. and Kim, K.J., 2020. Effects of carbon and silicon on electrical, thermal, and mechanical properties of porous silicon carbide ceramics. *Ceramics International*, Vol.46, Issue 10, pp.15594–15603. https://doi.org/10.1016/j.ceramint.2020.03.106.

Ksiazek, M., Tangstad, M. and Ringdalen, E., 2016. Five furnaces five different stories, *Silicon for the Chemical and Solar Industry XIII*, Kristiansand, Norway, 13-16 June 2016, pp.33-42.

Monsen, B., Lindstad, T. and Tuset, J., 1998. CO2 Emissions from the Production of Ferrosilicon and Silicon Metal in Norway, *56th Electric Furnace Conference*, New Orleans, United States of America, pp.371–378.

Ramos, D.C., Carneiro, A.D.C.O., Tangstad, M., Saadieh, R. and Pereira, B.L.C., 2019. Quality of Wood and Charcoal from Eucalyptus Clones for Metallurgical Use. *Floresta e Ambiente*, Vol.26, Special Issue 2. https://doi.org/10.1590/2179-8087.043518.

Ringdalen, E., 2018. SiC structures and SiC transformations in industrial Si- production. *Silicon for the Chemical and Solar Industry XIV*, Svolvær, Norway, 11-14 June 2018.

Sokhor, M.I. and Glukhov, V.P., 1965. Silicon Carbides with the Wurtzite Structure. *Sov. Phys. Crystallogr.*, Vol.10, pp.238–246.

Stabbforsmo, T. and Tangstad, M., 2026. Hot Strength of Coal and Charcoal by Spark Plasma Sintering Machine (To be published). *JOM*.

Steele, M.C. and Rosi, F.D., 1958. Thermal Conductivity and Thermoelectric Power of Germanium-Silicon Alloys. *Journal of Applied Physics*, Vol.29, Issue 11, pp.1517–1520. https://doi.org/10.1063/1.1722984.

Zhao, Y.X. and Spain, I.L., 1989. X-ray diffraction data for graphite to 20 GPa. *Physical Review B*, Vol.40, Issue 2, pp.993–997. https://doi.org/10.1103/PhysRevB.40.993.

Thea Stabbforsmo
PhD candidate, Norwegian University of Science and Technology

Thea Stabbforsmo is a PhD candidate at the Norwegian University of Science and Technology working with biocarbon in silicon production as a part of FME ZeMe. She holds a MSc in chemistry from NTNU.